5-2019

Modelling Palladium Decorated Graphene using Density Functional Theory to Analyze Hydrogen Sensing Application

Sameer Kulkarni

Modelling Palladium Decorated Graphene using Density Functional Theory to Analyze Hydrogen Sensing Application

By: Sameer Kulkarni

Acknowledgements

I would like to thank Dr. Wejinya for his continued throughout this entire research endeavor. I would also like to thank his graduate student, Yomi, for his support and expertise. Lastly, I appreciate Dr. Millet listening to my Thesis Defense and also providing some help with contacts in the Physics Department.

Abstract

Graphene is an exciting new material with many promising applications. One such application of graphene is gas sensing, when adsorbed with transition metals, notably Palladium. Therefore, it is of paramount importance to have appropriate ab initio calculations to calculate the various properties of graphene under different adsorbates and gasses. The first step in these calculations is to have a functioning base Density Functional Theory (DFT) model of pristine graphene decorated with Palladium. The computational methods described in this paper has yielded results for pristine graphene that have been confirmed many times in previous experimental and theoretical studies. Future work needs to consider different concentrations of H_2, Van der Waals correction, band graph calculations, and establishing a standardized set of parameters.

Keywords: Density Functional Theory, DFT, Graphene, Gas Sensors, Palladium, Hydrogen, Quantum ESPRESSO

Table of Contents

Table of Figures

1. Introduction

Hydrogen Sensors:

In the efforts of reducing CO_2 emissions and the search for viable renewable energy sources, Hydrogen (H_2) has emerged as a promising candidate [3]. Its pollution free usage (since combustion of H_2 produces pure water), availability, and future accessibility makes it an attractive choice to replace conventional fossil fuel based sources. Current uses of Hydrogen include highly efficient fuel cells [1] that have the potential to replace gasoline based engines, heat treatments of metals, and food processing [2]. For many of its applications, knowledge and control of concentration of H_2 is crucial to maintain high quality of the final product. Since H_2 is colorless, odorless, tasteless, and highly flammable, the need for a working H_2 sensor to detect leaks, concentration, or purity is necessary to ensure quality and safety.

Current H_2 sensors are either limited in measuring range (can only measure between a certain concentration range), accuracy percentage, response time, or the gas environment, which is the acceptable surroundings such as range of temperature or pressure values – in which the sensor can remain functional [4]. To account for shortcomings of the current sensors, research is being conducted on semiconductors with a wide band gap, as these materials would be more environmentally independent and robust. One such material is graphene – a single layer of carbon atoms arraigned in a hexagonal structure. Graphene, as a semiconductor [6], would give the added benefits of structural flexibility and unique beneficial electronic properties [5].

Graphene Based Gas Sensors

Graphene, a single 2 dimensional layer of carbon atoms arranged in a hexagonal structure, has spurred prodigious amounts of research into its unique electrical and mechanical properties. One such area of research is utilizing first principles calculations to analyze applications of graphene with respect to gas sensors. The sensors function by taking advantage of graphene's change in electrical properties (such as conductance) in presence of various gasses. Therefore, by finding a correlation in the change in the electrical property and gas concentration, one can use graphene as a gas sensor. As mentioned before, Graphene's large surface area, wide band gap, and structural flexibility make it a very promising candidate for gas sensing applications [5]. These sensors are also expected to be highly sensitive and are able to operate under a large temperature range, making them more robust than current commercially available sensors. However, the attraction of pristine graphene to many of the stable gasses such as hydrogen gas (H_2) or methane (CH_4) is very weak [8]. Therefore, introducing adsorbates and modifying pristine graphene chemically is necessary to increase the reactivity of graphene to surrounding gasses. Studies have shown that transition metals make good adsorbates to increase graphene's sensitivity. Specifically, Palladium (Pd) appears to be the most promising adsorbate for gas sensing and storage applications [9]. Therefore, a gas sensor comprised of a pristine graphene layer decorated with Pd with an electric device (such as a multimeter) to measure the conductance (or resistance) across the graphene layer can form the core for a graphene based gas sensor, as summarized in the Figure 1 below.

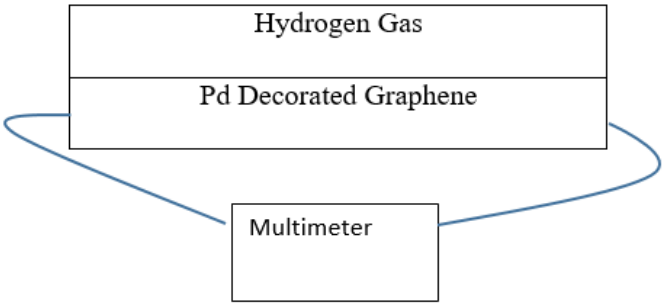

Figure 1 - Crude Representation of Graphene Based Hydrogen Gas Sensor

Producing a monolayer of graphene without defects is an incredibly difficult, expensive, and time consuming process [10]. Therefore, before conducting the experimental tests, simulations can be performed to "test" the different hypothesis to significantly reduce cost and time. At the atomic scale (10^{-12} to 10^{-9} m), *ab initio* methods can be performed to calculate the properties of the atoms involved. One such method is Density Functional Theory or DFT [11], which will be explored in depth in the section below.

2. Density Functional Theory

DFT is a form of a*b initio* (Latin for "from the beginning") calculation, which are methods that only assume the base properties of the atom and their position in the model. They do not contain any external information specifying the interactions between each atoms and only let the governing equation to guide the calculations. In the case of DFT, the governing equation is the Schrödinger's Equation, which describes the different quantum energy levels for a model and is a more physically accurate version of F = ma or Newton's second law. Therefore, the solution to the Schrödinger's Equation can be used to ascertain various properties of any quantum-mechanical system (which is why the equation is described as a state function for an atomistic model). However, finding an analytical solution of the Schrödinger's Equation for non-trivial systems is impossible and numerical techniques must be used to approximate the solution. DFT is an unique approach to approximate this solution through utilizing some unique properties of the Schrödinger's Equation with respect to electron density of the atoms in the model.

Schrödinger's Equation

$$H\Psi = E\Psi$$

Put simply, the Schrödinger's Equation can be written as above (Where H is the Hamiltonian operator, Ψ is the wave function, and E is the energy of the system). However, when applied to each individual atom, the linear partial differential equation translates into what is known as the "many body problem". An illustration of the Hamiltonian operator for the many body problem can be seen in the figure below.

$$\hat{H} = \overbrace{-\frac{\hbar^2}{2}\sum_I \frac{\nabla_I^2}{M_I}}^{\text{Nuclei K.E.}} + \overbrace{\frac{1}{2}\sum_{I\neq J}\frac{Z_I Z_J e^2}{4\pi\epsilon_0 |\mathbf{R_I}-\mathbf{R_J}|}}^{\text{Nucleus-Nucleus Interaction}} - \overbrace{\frac{\hbar^2}{2m}\sum_i \nabla_i^2}^{\text{Electrons K.E.}} + \underbrace{\frac{1}{2}\sum_{i\neq j}\frac{e^2}{4\pi\epsilon_0 |\mathbf{r_i}-\mathbf{r_j}|}}_{\text{Electron-Electron Interaction}} - \underbrace{\sum_{i,I}\frac{Z_I e^2}{4\pi\epsilon_0 |\mathbf{r_i}-\mathbf{R_I}|}}_{\text{Electron-Nucleus Interaction}}$$

Figure 2 - Hamiltonian Operator for the Many Body Problem [7]

The operator is split into 5 components:

1. Nuclei Kinetic Energy (K.E)
2. Electrons K.E

Kinetic Energy Contribution

3. Nucleus-Nucleus Interactions
4. Electron-Electron Interaction
5. Electron-Nucleus Interaction

Potential Energy Contribution

Each of these components contribute towards the total energy of the atomic model. Note that the H is only dependent on the positioning of the atoms (represented by **R**), their mass and other atom specific constants, and the total number of atoms (for the series summations). Therefore, this matches our expectation of an *ab initio* calculation.

Born – Oppenheimer Approximation

Put simply, the Born-Oppenheimer approximation [12] assumes that the kinetic energy of nuclei will be much smaller in magnitude compared to the kinetic energy of the electrons.

Therefore, the many body Hamiltonian operator (after some changes with cleaning staff) can be then be rewritten as in the figure below, where the kinetic energy of the nuclei is negligible and close to zero.

$$\hat{H}^{\mathrm{BO}} = \underbrace{-\frac{\hbar^2}{2m}\sum_i \nabla_i^2}_{\text{Electrons K.E.}} + \underbrace{\frac{1}{2}\sum_{i\neq j}\frac{e^2}{4\pi\epsilon_0\left|\mathbf{r_i}-\mathbf{r_j}\right|}}_{\text{Electron-Electron Interaction}} - \underbrace{\sum_{i,I}\frac{Z_I e^2}{4\pi\epsilon_0\left|\mathbf{r_i}-\mathbf{R_I}\right|}}_{\text{Electron-Nucleus Interaction}} + \underbrace{\frac{1}{2}\sum_{I\neq J}\frac{Z_I Z_J e^2}{4\pi\epsilon_0\left|\mathbf{R_I}-\mathbf{R_J}\right|}}_{\text{Nucleus-Nucleus Interaction}}$$

Figure 3 - Hamiltonian Operator after Born-Oppenheimer Approximation for the Many Body System [7]

Hohenberg – Kohn Theorems

The Hohenberg – Kohn theorems can be used to help solve the Hamiltonian. The first theorem is as stated:

First Theorem: ***The ground state energy from Schrödinger's Equation is a unique functional of the electron density***

Where a functional is a function that maps functions to other functions and the electron density is the probability distribution for electrons in the model. On its own, the first theorem does not shed too much knowledge into how to solve the Hamiltonian. However, when coupled with the second theorem, the theorems give us an approach to solve Schrödinger's Equation using the Kohn – Sahm equations.

Second Theorem: The electron density that minimizes the energy of the overall functional is the true electron density corresponding to the full solution of the Schrödinger's Equation.

Therefore, the Hamiltonian operator can be rewritten as shown below. Note that the equation does not contain any constants (such as the mass of the electrons, nuclei, or plank's constant). V_{ext} ($\mathbf{r_i}$) can be found uniquely through the electron density function (First theorem).

$$\hat{H} = -\frac{1}{2}\sum_i \nabla_i^2 + \frac{1}{2}\sum_{i \neq j} \frac{1}{|\mathbf{r_i} - \mathbf{r_j}|} + \sum_i V_{ext}(\mathbf{r_i})$$

Figure 4 - Replacing the Electron Nucleus and Nucleus Nucleus Interactions by applying an External Potential [7]

This formulation leads to the Kohn-Sham approach, which solve the Kohn-Sham equations, which is shown below. Note that these equations do not contain any interactions (at least, explicitly in the formula) between the particles and replaces the interactions from the Hamiltonian with a non-interacting systems of equations by using the electron density function or n($\mathbf{r}$).

$$E[n] = F[n] + \int \mathrm{d}^3\mathbf{r}\, V_{ext}(\mathbf{r}) n(\mathbf{r})$$

Where

$$F[n] = \underbrace{T_s[n]}_{\text{K.E.}} + \underbrace{d^3\mathbf{r}\, d^3\mathbf{r}' \frac{n(\mathbf{r})\, n(\mathbf{r}')}{|\mathbf{r} - \mathbf{r}'|}}_{\text{Hartree}} + \underbrace{E_{xc}[n(\mathbf{r})]}_{\text{Exchange-Correlation}}$$

Figure 5 - Kohn-Sham Equations [7]

Exchange Correlation

Since calculating the kinetic energy of the particles is not possible through analytical methods, an exchange correlation is used to find this energy. The exchange correlation (XC) contains approximations about the electron density of the atom by using different techniques. The two most popular XC are Local Density Approximation (LDA) and Gradient Density Approximation (GGA).

Local Density Approximation

Assumes the electron density of an atom in the local area of a point remains constant. The size of the local area is determined by the integration grid used in the calculations. There are many published LDAs online, the most popular being the Perdew Zunger parametrization [13].

Generalized Gradient Approximation

This approximation also assumes a constant electron density in a local area. However, it to calculate this value, it uses the local electron density and its local gradient to get an average value. Note that just because GGA requires more information does not mean that it is more accurate when compared to LDA. Most popular GGAs are Perdew-Burke-Ernzerhof.

Self-Consistent Calculation Steps

Now, we can define an approach to solve the Kohn-Sham equations for a many body problem. These steps are:

1. Guess an initial electron density
2. Use this to solve the Kohn – Sham Equations
3. Calculate a new electron density

$$n_{KS}(\boldsymbol{r}) = 2 * \psi(\boldsymbol{r})\psi^{*}(\boldsymbol{r})$$

4. Compare new density to old density. Stop if change is within specified tolerances or if the calculation as achieved “self-consistence”.

3. Computational Details

An open source package Quantum ESPRESSO [14] was utilized to perform all of the calculations. These were performed by parallelizing the routines and running them on a cluster computer network [15]. XCrysDen [16], an atomic model visualization software was used to create supercells and get visual figures of the models. A plane-wave periodicity (the cell defined repeats in all directions as directed) assumption is used to calculate bulk properties. The specific details for each of the model are discussed in the following section:

Computational Model Details

A. Pristine Graphene Unit Cell

To calculate the cell parameters for graphene, the standard hexagonal and trigonal crystalline structure was used with two carbon atoms in the unit cell with the crystal coordinates (1/3, 2/3, 0) and (2/3, 1/3, 0). A GGA exchange correlation within the PBE framework for the pseudopotentials were utilized. The cut-off energy for the plane-wave basis expansion was 60 Ry for the wave function and 600 Ry for the charge density. The force and energy convergence threshold was set to 10-4 and 10-5 Ry respectively. A variable cell relaxation calculation (restricted to ‘x’ and ‘y’ dimensions since graphene is 2 Dimensional) was performed using Broyden-Fletcher-Goldfarb-Shanno [4] (BFGS) scheme to determine the cell parameters until the force threshold was satisfied. The results were then used to perform additional relaxation and energy calculations. All calculations used a Monkhorst-Pack grid of 12x12x1 k-points to sample the Brillouin zone. A Marzari-Vanderbuilt smearing of 0.001 Ry was also utilized.

B. Pristine and Pd Decorated Graphene Supercell

The results from the calculations for pristine graphene on a unit cell were used to build a 4x4 graphene supercell with 32 carbon atoms as shown in the figure below.

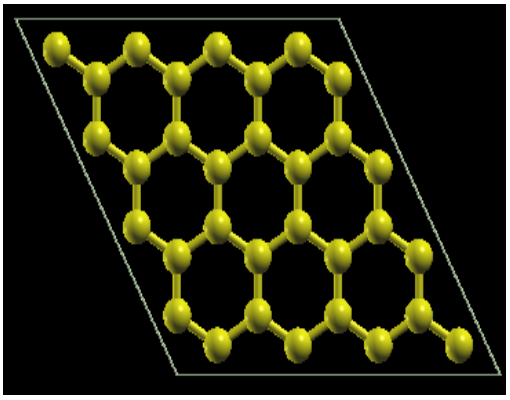

Figure 6 - A 4x4 32 Atom Graphene Supercell

The parameters for the supercell were changed significantly from before for better accuracy and adherence to existing publications. Ultrasoft (Vanderbuilt) pseudopotentials were used that also used the GGA exchange correlation PBE framework. The cut-off energy for the plane-wave basis expansion was changed to 50 Ry for the wave function and 500 Ry for the charge density. The force and energy threshold remained the same at 10^{-4} and 10^{-5} Ry respectively. Similar to before, a variable cell calculation was performed, which allowed for z variation for the Pd decorated graphene. The results were then used to perform another relaxation calculation followed by the ground state energy calculation.

These calculations were then repeated by putting H_2 molecule on top of the pristine graphene to confirm whether or not H_2 is attracted to pristine graphene or not.

4. Results

A. Pristine Graphene Unit Cell

The results of this calculations were well within reported theoretical and experimental values [9]. The C-C bond length was 1.425 Å with a lattice constant of 2.47 Å. The following cell parameters (3 vectors that define the periodicity of the unit cell) were also found and are shown in Figure below.

```
crystal axes: (cart. coord. in units of Angstroms)
        a(1) = (   2.468612   0.000000   0.000000 )
        a(2) = (  -1.234341   2.137940   0.000000 )
        a(3) = (   0.000000   0.000000  29.528090 )
```

Figure 7 - Cell Parameters for Graphene

B. Pristine and Pd Decorated Graphene

The supercell calculations for pristine graphene also yielded results consistent with previous studies. For example, the total energy for the pristine graphene supercell was -4966 eV compared to -4963 eV in [3]. The introduction of Pd atom on top of a bridge site of a C-C atom, as shown in Figure 8 below, caused perturbations of the graphene atoms in the z direction, taking away its 2-D property. The final cell parameters for this model are also presented in the Figure 9 below.

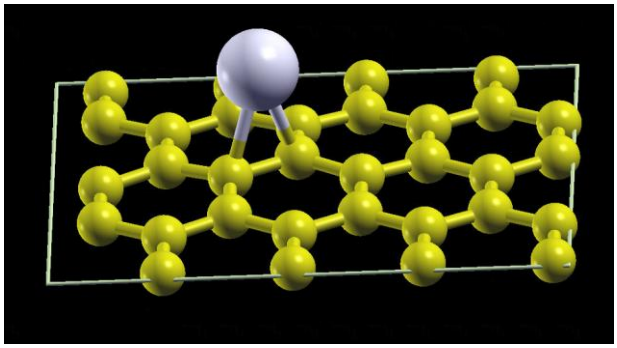

Figure 8 - Graphene Supercell with Pd Atom At Bridge Site

```
CELL_PARAMETERS (units in angstrom)
a(1) = 9.878390779      -0.077462998     0.033696240
a(2) = 0.061436706      8.576993256      0.101183908
a(3) = 0.029689796      0.081963724      10.612649898
```

Figure 9 - Cell Parameters for Graphene Supercell with Pd Atom

The calculations for H_2 on top of pristine graphene are still ongoing and will need further analysis done before reporting the results. However, early iterations of the output shows that H_2, when deposited 2 Angstrom away (see figure below) from the graphene layer, tends to go away from the layer (to around 3.3 Angstrom right now).

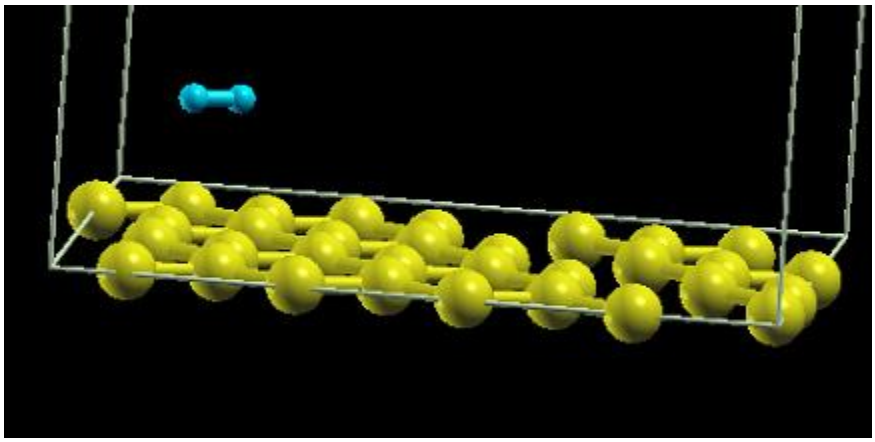

Figure 10 - Hydrogen Molecule on Top of Pristine Graphene

5. Conclusion and Future Work

The results of the pristine graphene matching the experimental and other theoretical values confirms that the methodology used and followed yields accurate results. However, a lot of work still needs to be done before we can fully gage the efficacy of graphene as a hydrogen sensor. The amount of work needed is listed below:

1. Incorporating Van der Waals Forces

   Since DFT only concerns itself with the electron interactions locally, it fails to account for the Van der Waals forces present in our models. Therefore, a correction needs to be introduced into Quantum ESPRESSO to enable a dispersion correction mechanism to yield more accurate answers.

2. Performing simulations with different concentrations of H_2

   Having solutions for different concentrations of H_2 will allow us to find the correlation between the electrical conductivity of Pd decorated Graphene and the concentration of H_2. Once this relationship is established, it can be backtracked and used in the sensor to report the concentration of H_2.

3. Finding Band Graphs

   To find the electrical conductivity across the graphene layer, a band graph must be calculated. To achieve this, a very fine k point grid must be used, along with defining a pathway in the Brillouin zone

4. Establishing a set of standardized parameters

   To ensure any comparability between simulations and different studies, a standardized set of parameters for graphene related calculations needs to be established to streamline the process and get more reliable results.

6. References

[1] Haseli, Y. (2018). Maximum conversion efficiency of hydrogen fuel cells. International Journal of Hydrogen Energy, 43(18), 9015–9021. https://doi.org/10.1016/j.ijhydene.2018.03.076

[2] Gandia, L., Arzamendi, G. & guez, P. (2013). *Renewable hydrogen technologies : production, purification, storage, applications and safety*. Amsterdam: Elsevier Science.

[3] Balat, M., & Balat, M. (2009). Political, economic and environmental impacts of biomass-based hydrogen. International Journal of Hydrogen Energy, 34(9), 3589–3603. https://doi.org/10.1016/j.ijhydene.2009.02.067

[4] Hübert, T., Boon-Brett, L., Black, G., & Banach, U. (2011). Hydrogen sensors – A review. Sensors and Actuators B: Chemical, 157(2), 329–352. https://doi.org/10.1016/j.snb.2011.04.070

[5] Castro Neto, A. H., Guinea, F., Peres, N. M. R., Novoselov, K. S., & Geim, A. K. (2009). The electronic properties of graphene. Reviews of Modern Physics, 81(1), 109–162. https://doi.org/10.1103/revmodphys.81.109

[6] Hicks, J., Tejeda, A., Taleb-Ibrahimi, A., Nevius, M. S., Wang, F., Shepperd, K., … Conrad, E. H. (2012). A wide-bandgap metal–semiconductor–metal nanostructure made entirely from graphene. Nature Physics, 9(1), 49–54. https://doi.org/10.1038/nphys2487

[7] Elgammal, K. (2018). Density Functional Theory Calculations for Graphene-based Gas Sensor Technology (PhD dissertation). Stockholm, Sweden, 2018. Retrieved from http://urn.kb.se/resolve?urn=urn:nbn:se:kth:diva-221639

[8] Intrinsic Response of Graphene Vapor Sensors, Yaping Dan, Ye Lu, Nicholas J. Kybert, Zhengtang Luo, and A. T. Charlie Johnson, Nano Letters 2009 9 (4), 1472-1475, DOI: 10.1021/nl8033637

[9] Sh. Nasresfahani, R. Safaiee, M.H. Sheikhi, Influence of Pd/Pd2 decoration on the structural, electronic and sensing properties of monolayer graphene in the presence of methane molecule: A dispersion-corrected DFT study, Surface Science, Volume 662, 2017, Pages 93-101, ISSN 0039-6028, https://doi.org/10.1016/j.susc.2017.04.002.

[10] Elgammal, K. (2018). Density Functional Theory Calculations for Graphene-based Gas Sensor Technology (PhD dissertation). Stockholm, Sweden, 2018. Retrieved from http://urn.kb.se/resolve?urn=urn:nbn:se:kth:diva-221639

[11] Steinhauser, Martin O, and Stefan Hiermaier. "A review of computational methods in materials science: examples from shock-wave and polymer physics." *International journal of molecular sciences* vol. 10,12 5135-216. 1 Dec. 2009, doi:10.3390/ijms10125135

[12] M. Born and K. Huang, *Dynamical Theory of Crystal Lattices*, International series of monographs on physics (Clarendon Press, 1998).

[13] J. P. Perdew and A. Zunger, Phys. Rev. B 23, 5048 (1981).

[14] P. Giannozzi, S. Baroni, N. Bonini, M. Calandra, R. Car, C. Cavazzoni, D. Ceresoli, G. L. Chiarotti, M. Cococcioni, I. Dabo, A. Dal Corso, S. Fabris, G. Fratesi, S. de Gironcoli, R. Gebauer, U. Gerstmann, C. Gougoussis, A. Kokalj, M. Lazzeri, L. Martin-Samos, N. Marzari, F. Mauri, R. Mazzarello, S. Paolini, A. Pasquarello, L. Paulatto, C. Sbraccia, S. Scandolo, G. Sclauzero, A. P. Seitsonen, A. Smogunov, P.

Umari, R. M. Wentzcovitch, J.Phys.:Condens.Matter 21, 395502 (2009) http://dx.doi.org/10.1088/0953-8984/21/39/395502

[15] University of Arkansas, Arkansas High Performance Computing Center, https://hpc.uark.edu

Appendix – Quantum Espresso Input Codes

Graphene 32 Atom Supercell Variable Cell

```
&CONTROL
                    title = 'GrapheneOnly32_VCRelax' ,
               calculation = 'vc-relax' ,
               max_seconds = 21000,
                   outdir = 'GrapheneOnly32_VCRelax_Temp' ,
                pseudo_dir = './' ,
              restart_mode = 'restart' ,
                   prefix = 'grapheneOnly32_VCRelax' ,
                verbosity = 'low' ,
             etot_conv_thr = 1.0D-5 ,
             forc_conv_thr = 1.0D-4 ,
                    nstep = 50 ,
/
 &SYSTEM
                    ibrav = 1,
                celldm(1) = 20,
                    celldm(2) = 1,
                    celldm(3) = 12,
                   nat = 32,
                   ntyp = 1,
                ecutwfc = 50 ,
                ecutrho = 500 ,
               occupations = 'smearing' ,
                degauss = 0.005 ,
/
 &ELECTRONS
```

```
        electron_maxstep = 100,
              conv_thr = 1.0d-8 ,
            mixing_mode = 'local-TF' ,
            mixing_beta = 0.7 ,
/
&IONS
             ion_dynamics = 'bfgs' ,
            ion_positions = 'default' ,
                 upscale = 100 ,
/
&CELL
            cell_dynamics = 'bfgs' ,
             cell_factor = 2.0 ,
             cell_dofree = '2Dxy' ,
/

ATOMIC_SPECIES
   C   12.01000  c_pbe_v1.2.uspp.F.UPF

ATOMIC_POSITIONS angstrom
C        0.000000000   2.080669841   0.000000000
C        1.230336033   1.370334921   0.000000000
C        2.460673050   2.080669841   0.000000000
C        3.691009083   1.370334921   0.000000000
C        4.921346100   2.080669841   0.000000000
C        6.151682133   1.370334921   0.000000000
C        7.382019150   2.080669841   0.000000000
C        8.612355183   1.370334921   0.000000000
C        -1.230336525  4.211674111   0.000000000
C        -0.000000492  3.501339190   0.000000000
```

C 1.230336525 4.211674111 0.000000000
C 2.460672558 3.501339190 0.000000000
C 3.691007575 4.211674111 0.000000000
C 4.921345608 3.501339190 0.000000000
C 6.151682625 4.211674111 0.000000000
C 7.382018658 3.501339190 0.000000000
C -2.460673050 6.342678371 0.000000000
C -1.230337017 5.632343451 0.000000000
C 0.000000000 6.342678371 0.000000000
C 1.230336033 5.632343451 0.000000000
C 2.460673050 6.342678371 0.000000000
C 3.691009083 5.632343451 0.000000000
C 4.921346100 6.342678371 0.000000000
C 6.151682133 5.632343451 0.000000000
C -3.691009575 8.473682641 0.000000000
C -2.460673452 7.763347720 0.000000000
C -1.230336525 8.473682641 0.000000000
C -0.000000492 7.763347720 0.000000000
C 1.230336525 8.473682641 0.000000000
C 2.460672558 7.763347720 0.000000000
C 3.691009575 8.473682641 0.000000000
C 4.921345608 7.763347720 0.000000000

K_POINTS automatic

18 18 1 0 0 0

Graphene and Palladium Variable Cell Relax Input Code

```
&CONTROL
                    title = 'GrapheneOnly32_VCRelax' ,
               calculation = 'vc-relax' ,
               max_seconds = 21000,
                   outdir = 'GrapheneOnly32_VCRelax_Temp' ,
                pseudo_dir = './' ,
              restart_mode = 'restart' ,
                   prefix = 'grapheneOnly32_VCRelax' ,
                verbosity = 'low' ,
             etot_conv_thr = 1.0D-5 ,
             forc_conv_thr = 1.0D-4 ,
                    nstep = 50 ,
/
 &SYSTEM
                    ibrav = 1,
                celldm(1) = 20,
                    celldm(2) = 1,
                    celldm(3) = 12,
                   nat = 32,
                  ntyp = 1,
                ecutwfc = 50 ,
                ecutrho = 500 ,
               occupations = 'smearing' ,
                degauss = 0.005 ,
/
 &ELECTRONS
          electron_maxstep = 100,
                conv_thr = 1.0d-8 ,
```

```
   mixing_mode = 'local-TF' ,
   mixing_beta = 0.7 ,
/
&IONS
   ion_dynamics = 'bfgs' ,
  ion_positions = 'default' ,
      upscale = 100 ,
/
&CELL
  cell_dynamics = 'bfgs' ,
   cell_factor = 2.0 ,
   cell_dofree = '2Dxy' ,
/

ATOMIC_SPECIES
  C  12.01000  c_pbe_v1.2.uspp.F.UPF

ATOMIC_POSITIONS angstrom
C       0.000000000   2.080669841   0.000000000
C       1.230336033   1.370334921   0.000000000
C       2.460673050   2.080669841   0.000000000
C       3.691009083   1.370334921   0.000000000
C       4.921346100   2.080669841   0.000000000
C       6.151682133   1.370334921   0.000000000
C       7.382019150   2.080669841   0.000000000
C       8.612355183   1.370334921   0.000000000
C       -1.230336525  4.211674111   0.000000000
C       -0.000000492  3.501339190   0.000000000
C       1.230336525   4.211674111   0.000000000
C       2.460672558   3.501339190   0.000000000
```

C 3.691007575 4.211674111 0.000000000
C 4.921345608 3.501339190 0.000000000
C 6.151682625 4.211674111 0.000000000
C 7.382018658 3.501339190 0.000000000
C -2.460673050 6.342678371 0.000000000
C -1.230337017 5.632343451 0.000000000
C 0.000000000 6.342678371 0.000000000
C 1.230336033 5.632343451 0.000000000
C 2.460673050 6.342678371 0.000000000
C 3.691009083 5.632343451 0.000000000
C 4.921346100 6.342678371 0.000000000
C 6.151682133 5.632343451 0.000000000
C -3.691009575 8.473682641 0.000000000
C -2.460673452 7.763347720 0.000000000
C -1.230336525 8.473682641 0.000000000
C -0.000000492 7.763347720 0.000000000
C 1.230336525 8.473682641 0.000000000
C 2.460672558 7.763347720 0.000000000
C 3.691009575 8.473682641 0.000000000
C 4.921345608 7.763347720 0.000000000

K_POINTS automatic
18 18 1 0 0 0

Graphene 32 Atom Supercell – Self Consistent Ground State Energy Calculation

```
&CONTROL
                    title = 'GrapheneOnly32_Scf' ,
               calculation = 'scf' ,
               max_seconds = 20000,
                   outdir = 'GrapheneOnly32_Scf_Temp' ,
                pseudo_dir = './' ,
                   prefix = 'grapheneOnly32_Scf' ,
                 verbosity = 'low' ,
              etot_conv_thr = 1.0D-5 ,
              forc_conv_thr = 1.0D-4 ,
 /
 &SYSTEM
                    ibrav = 0,
                      celldm(1) = 20,
                     nat = 32,
                    ntyp = 1,
                  ecutwfc = 50 ,
                  ecutrho = 500 ,
               occupations = 'smearing' ,
                  degauss = 0.005 ,
/
 &ELECTRONS
          electron_maxstep = 100,
                 conv_thr = 1.0d-9 ,
              mixing_mode = 'local-TF' ,
              mixing_beta = 0.7d0 ,
/
```

ATOMIC_SPECIES

C 12.01000 c_pbe_v1.2.uspp.F.UPF

ATOMIC_POSITIONS (angstrom)

C -0.139368240 1.131788998 0.000000000
C 1.071345955 0.382527741 0.000000000
C 2.323924764 1.059484330 0.000000000
C 3.534610136 0.310174254 0.000000000
C 4.787183585 0.987144193 0.000000000
C 5.997898074 0.237870533 0.000000000
C 7.250471160 0.914812805 0.000000000
C 8.461149234 0.165468639 0.000000000
C -1.308190740 3.305913135 0.000000000
C -0.097509625 2.556594476 0.000000000
C 1.155070446 3.233553939 0.000000000
C 2.365779760 2.484293494 0.000000000
C 3.618354240 3.161262318 0.000000000
C 4.829033116 2.411956118 0.000000000
C 6.081610583 3.088910193 0.000000000
C 7.292316459 2.339623525 0.000000000
C -2.477051650 5.480004800 0.000000000
C -1.266346188 4.730718153 0.000000000
C -0.013768771 5.407672109 0.000000000
C 1.196909263 4.658365846 0.000000000
C 2.449483762 5.335334677 0.000000000
C 3.660193398 4.586074190 0.000000000
C 4.912773383 5.263033803 0.000000000
C 6.123455462 4.513715106 0.000000000
C -3.645884828 7.654159676 0.000000000
C -2.435206320 6.904815513 0.000000000

C -1.182633364 7.581757689 0.000000000

C 0.028080236 6.832484083 0.000000000

C 1.280653750 7.509453907 0.000000000

C 2.491338817 6.760143838 0.000000000

C 3.743917549 7.437100449 0.000000000

C 4.954632582 6.687839212 0.000000000

K_POINTS automatic

18 18 1 0 0 0

CELL_PARAMETERS {alat}

0.930982942 -0.027341296 0.000000000

0.023727652 0.808022146 0.000000000

0.000000000 0.000000000 1.000000000